



The Investigation of Modeling Material Behavior in Autofrettaged Tubes Made from Aluminium Alloys

K. Aliakbari*, Kh. Farhangdoost

Department of Mechanical Engineering, Ferdowsi University of Mashhad, Mashhad, Iran

PAPER INFO

Paper history:

Received 25 September 2012

Accepted in revised form 07 November 2013

Keywords:

Thick-Walled Tube

Autofrettage

Nonlinear Mathematical Model

Bauschinger Effect

Aluminum Alloys

A B S T R A C T

In this research, a nonlinear strain hardening mathematical model is proposed for 7075 aluminium alloy (A7075). Uniaxial tension-compression experimental data are used to figure out a suitable model to study the Bauschinger effect factor, BEF. Hence, uniaxial tension-compression tests on specimens having 12.5 mm and 6 mm diameters were carried out by an Instron servohydraulic machine and the results were compared. In this paper several factors including Young's modulus, the amount of offsets to determine yield point and BEF were studied. Besides, BEF in the aluminium tubes made from A5083 and A7075 alloys were compared. This model will be employed to predict residual stress and fatigue life in autofrettaged tubes.

doi: 10.5829/idosi.ije.2014.27.05b.17

1. INTRODUCTION

There are many industrial uses of thick-walled cylindrical pressure vessels such as power plant boilers, nuclear and chemical reactors, gun barrels and reactor pressure vessels. These are now used in renewable energy industries and also food preparation industries. Thick-walled cylinders are not only resisting against high internal pressures, but also are bearing pressure fluctuations, heat shock, and a corrosive environment, which all cause crack initiation and fatigue crack growth [1]. Many comprehensive researches have been carried out on crack propagation in thick-walled pressure tubes reflecting its importance [2].

The pressure in tubes is mostly of cyclic type and can cause cracks due to the fatigue which in turn causes the leakage of the under-pressure fluid, or eventually leads to the bursting of tubes [3]. One of the effective methods of increasing the pressure capacity in thick-walled tubes is applying the process of autofrettage. In this method, making the plastic zone of the walls up to a

certain radius is done by an internal pressure (hydraulic autofrettage or swage autofrettage). After releasing the internal pressure, what remains is residual stress distribution in the tube that consequently increases the loading capacity and resistance against the growing rate of internal cracks. As the autofrettage process is affected by a loading-unloading cycle, the material behavior should be dealt with carefully [4]. The first analytical model of the autofrettage process was proposed by Hill [5] in 1950. This model assumes plane strain, elastic-perfectly plastic material, von Mises yield criterion and the condition incompressibility without considering the Bauschinger effect factor. The ratio of the decreased yield stress in reversed loading to the initial yield stress from a certain amount of plastic deformation is called Bauschinger effect factor (BEF). It was discovered by Bauschinger [6] in 1881. The autofrettage process is affected by plastic deformation of loading-unloading cycle. Hence, to analyze the autofrettage process it is essential to calculate the BEF accurately. Perry et al. [7] have generalized the Bauschinger effect (BE) to other parts of unloading behavior and attribute them to the effects including variable Young's modulus related to unloading phase

*Corresponding Author Email: karimaliakbari@yahoo.com (K. Aliakbari)

and nonlinear hardening behavior after reversed yield point.

The researchers such as Parker et al. [8], Farrahi et al. [9], Troiano et al. [10], Megahed and Abbas [11], Huang and Cui [12] tried to present mathematical models for the behavior of steels such as ASTM A723, HB7 and DIN1.6959. On the other hand, Jahed et al. [13, 14] examined the autofrettage process directly using the results of experimental data and without mathematical modeling.

The main purpose of this paper is to present mathematical model description of A7075 in loading-unloading phases which follows the ASTM B210M-05 standard and is used in pressure cylindrical vessels. Despite various studies on several steels, in the knowledge of authors, no work may be addressed in the modeling of loading-unloading behavior of A7075. In addition, such important cases like sample size, the amount of offsets to determine yield point and BEF have been tested. Also, the effect of plastic strain on Young's modulus changes has been studied in this paper. Besides, the BEF in A7075 was compared with 5083 aluminum alloy (A5083), both of which are used in high pressure tubes.

2. MATERIAL AND EXPERIMENTAL TEST PROCEDURE

The material used in this research is A7075. Its chemical composition is determined based on the ASTM E1251-07:2010 standard that is equivalent to A7075 in USA AA standard. The chemical compositions of both A7075 and A5083 alloys [15] are similar but their chemical composition quantities are different (see Table 1).

The mechanical properties of A7075 alloy used in this study follow the aging treatment of T73. The mechanical properties of A5083 [15] and A7075 alloys have been listed in Table 2 according to the ASTM B210M-05 that is a standard for aluminum and aluminum-alloy seamless tubes.

To study the loading-unloading behavior of A7075, the experimental results of uniaxial tension-compression tests are used. To carry out these tests, tension-compression test specimens were prepared. Pieces of 165 mm length were cut from an aluminum rod having 60 mm diameter. Then, the pieces were divided into four equal parts and finally, after careful machining by a CNC lathe, twenty specimens 12.5 mm in diameter and ten other specimens having 6 mm diameter were prepared. These specimens then were used for tests to determine the mechanical properties and material modeling. The dimensions of specimens having 12.5 mm diameter are improved dimensions based on ASTM E8M-97a standard that were prepared by Farrahi et al.

[9] (see Figure 1). This standard determines the standard test method of metallic materials. The important machining characteristic of A7075 was that the chips were broke easily, leading to very good finished surfaces.

A 30 tons Instron servohydraulic machine of model 8502 was used for experimental tests. This machine has a high level of accuracy for such tests. The methods of the experimental tests were similar to the methods done in Refs. [7, 9-10] in the cyclic control of load and the results were recorded in load-displacement mode. The sampling number per second was 2. Displacement in specimens having 12.5 mm diameter was measured by extensometer having the evaluation length of 27.5 mm. The same procedure was followed for the 6 mm diameter specimens. .

TABLE 1. Chemical compositions (wt %) of A7075 and A5083 [15]

Element	A7075 (current work)	A7075 (standard)	A5083
Al	Base	Base	Base
Si	0.36	≤0.40	≤0.40
Fe	0.37	≤0.50	≤0.40
Cu	1.3	1.2-2.0	≤0.1
Mn	0.22	≤0.30	0.4-1
Mg	2.11	2.1-2.9	4-4.9
Cr	0.19	0.18-0.28	0.05-0.25
Ni	0.013	-	-
Zn	5.21	5.1- 6.1	≤0.25
Ti	0.031	≤0.20	≤0.75
Pb	0.028	-	-
V	0.007	-	-
Zr	0.003	-	-

TABLE 2. Mechanical properties of A5083 [15] and A7075

Materials	A7075 (current work)	A7075 (Standard)	A5083
0.2% Yield strength (MPa)	450	≥385	100.5
UTS (MPa)	500	≥455	-
% Elongation	12.9	≥12	-
% Reduction in area	26.73	-	-
Young's modulus (GPa)	70.19	71	70.3

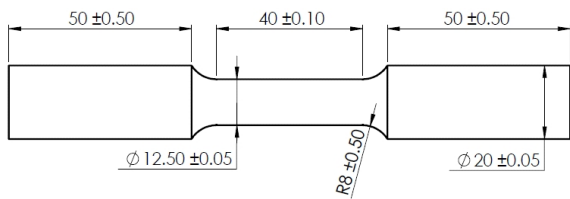


Figure 1. The geometrical dimensions of specimens having 12.5 mm diameter [9].

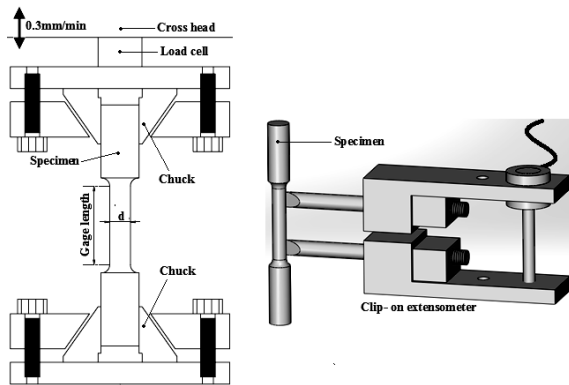


Figure 2. Instron servohydraulic machine and a typical extensometer

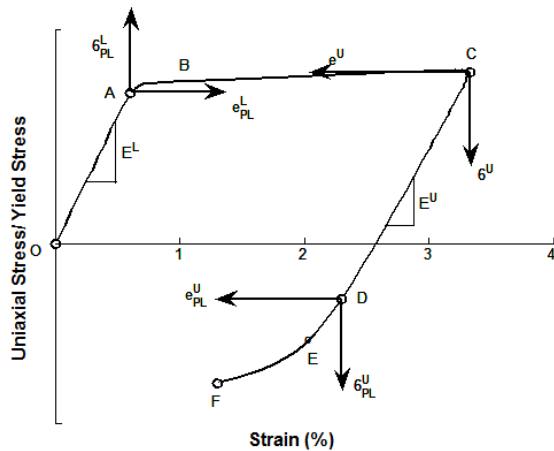


Figure 3. The stress-strain curve describing the material behavior in loading-unloading and reloading.

Experiments were carried out at the rate of 0.30 mm per minute. Figure 2 shows the Instron servohydraulic machine and a typical extensometer used in the experiments.

3. ANALYSIS OF THE THEORY

Figure 3 illustrates important sections of loading and unloading phases in uniaxial tension-compression test of A7075 alloy used for modeling the behavior of material

in the analysis of autofrettage process. The loading phase (tension) includes linear elastic behavior O-A, strain hardening A-B-C and unloading phase (compression) contains linear elastic behavior C-D and nonlinear hardening D-E-F. When a tube undergoes autofrettage process, in the loading and unloading phases, the equivalent stresses in the tubes take the paths of O-A-B-C and C-D-E-F, respectively. Therefore, there are series of cycles O-A-B-C-D-E-F each of which is a function of initial plastic strain and radial direction defining the equivalent stress required for the analysis of autofrettage process [8, 9].

The stress-strain relationships can be expressed in loading and unloading phases as follows:

3. 1. Linear Loading (O-A) From point O to the yield point A, the material has an elastic behavior and follows Hook's law (see Figure 3).

$$\sigma^L = E^L \varepsilon^L \tag{1}$$

where σ^L , ε^L and E^L are normal stress, normal strain and Young's modulus in loading, respectively.

3. 2. Nonlinear Loading (A-B-C) In this section, the plasticity dominates with nonlinear hardening behavior. A7075 like many other materials has nonlinear behavior within A-C, but it has linear strain hardening behavior in B-C section with very low slope.

Parker et al. [8] presented the following equation to describe plastic behavior in $e_{PL}^L A \sigma_{PL}^L$ coordinate system (see Figure 3).

$$\sigma_{PL}^L / \sigma_Y = B_1 \tanh(B_2 e_{PL}^L) + B_3 e_{PL}^L \tag{2}$$

where σ_{PL}^L and e_{PL}^L are normal stress and strain in coordinate system $(e_{PL}^L A \sigma_{PL}^L)$, respectively and σ_Y is yielding strength. Note that e_{PL}^L shows plastic strain in percent. The first part of the equation is nonlinear phase of A-B and the second part is linear hardening strain of B-C. B_1 , B_2 and B_3 , are factors of Equation (2) that depends on material behavior.

3. 3. Linear Unloading (C-D) The material behavior from point C to point D is elastic and it follows Hook's law. Using the new coordinate system $(\varepsilon^U C \sigma^U)$, the equation is as follows:

$$\sigma^U = E^U \varepsilon^U \tag{3}$$

σ^U , ε^U and E^U are normal stress, normal strain and Young's modulus in unloading phase, respectively. E^U is a function of e_{PL}^{L*} , that increases when e_{PL}^{L*} decreases, and e_{PL}^{L*} is maximum initial plastic strain.

This is, in fact, the maximum plastic strain which is created in the specimen before unloading phase. In all presented equations in this paper, e_{PL}^{L*} is in percent.

3. 4. Nonlinear Unloading (D-E-F) Modeling the nonlinear hardening behavior in regime D-E-F for high strength materials is a difficult task. Parker et al. [8, 10] investigated the asymptote model presented by Chaboche to describe the behavior of steels in this regime. They proposed an improved asymptote model having Bauschinger effect. This model has two important characteristics. Firstly, it has the potential to make the required fit on total curve series of this part which are functions of initial plastic strain. Secondly, for large amounts of compression strain, it moves toward a band in the form of asymptote. Also, Farrahi et al. [9] presented mathematical model to describe steel behavior DIN1.6959 in this regime.

Considering these two important characteristics given by Parker et al. [8], the mentioned complex behavior of nonlinear unloading maybe modeled using Equation (4).

$$\sigma_{PL}^L / \sigma_Y = (1 + B_1 - BEF) \tanh(\gamma e_{PL}^U) + BEF + B_3 e_{PL}^U \quad (4)$$

where σ_{PL}^U and e_{PL}^U are normal stress and strain in coordinate system $(e_{PL}^U D\sigma_{PL}^U)$, respectively. B_1 and B_3 are factors of Equation (2). Moreover, BEF and γ are both functions of e_{PL}^{L*} . BEF is Bauschinger effect factor and γ is nonlinear hardening strain. Equation (4) was used frequently by Parker et al. [8] for modeling A723 and several other steels.

4. EXPERIMENTAL RESULTS AND DISCUSSION

4. 1. Investigating the Young’s Modulus in Loading and Unloading Phases

Many researchers have shown that the stress-strain curve in unloading phase is nonlinear; consequently, Young’s modulus is not a fixed quantity. Various methods of determining Young’s modulus were examined by Perry et al. [7]. They introduced the average Young’s modulus method for modeling the practical behavior of material. To determine the average Young’s module, first tangential modulus in different points along the entire loading-unloading curve is calculated as follows:

$$(E_{tg})_i = \frac{\sigma_{i+1} - \sigma_{i-1}}{\varepsilon_{i+1} - \varepsilon_{i-1}} \quad (5)$$

The fact that the two ends of the stress-strain curve of loading and unloading phases are mostly nonlinear caused 5 percent of beginning and end of the the curve

to be deleted, and calculated average tangential modulus along with the rest of the curve. In this research, the method of average Young’s modulus is used to calculate Young’s modulus in loading and unloading phases.

Several specimens, each loaded separately with a unique strain and then subjected to unloading phase were included to examine loading-unloading Young module. These testes were carried out up to total strain of 4.3% (i.e., elastic strain+ plastic strain). Figure 4 illustrates the results of single-cycle tests in a graph where each test has been done independently on one specimen.

The Young’s modulus in loading and unloading phases was investigated for A723, HY180 and PH 13-8Mo Steels by Parker et al. [8] and for DIN1.6959 steel by Farrahi et al. [9].

Considering these works, the following equation may be concluded to describe the proposed fit to the experimental data of the A7075 in which E^U has been normalized.

$$E^U / E^L = 1.0 - 0.1728 \tanh(0.4172(e_{PL}^{L*})^{0.8166}) \quad (6)$$

Figure 5 shows the experimental results of A7075 as well as the proposed fit for E^U / E^L versus initial plastic strain. As Figure 5 shows, when the initial plastic strain increases, the ratio E^U / E^L decreases. The main difference is in the loading results of the Young’s modulus. This difference is less in the 6 mm specimen compared to the 12.5 mm specimen, and is negligible. Farrahi et al. [15] investigated the modulus of elasticity of 5083 aluminum alloy came up with the same quantities in loading and unloading phases, while in many steels like A723, PH13 [10] and DIN1.6959 the decrease in elastic modulus is more in unloading phase compared to the loading phase [9].

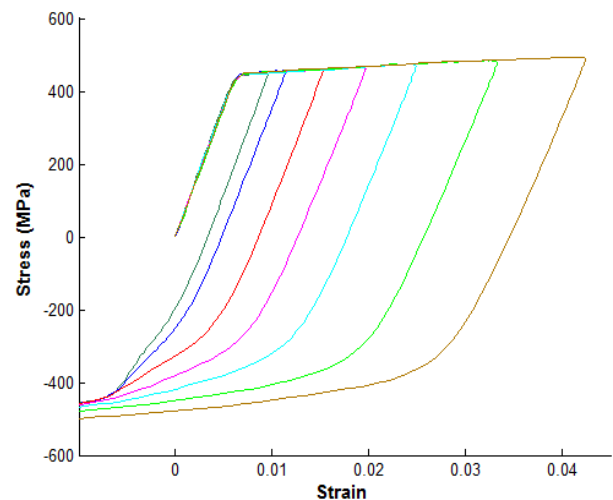


Figure 4. Engineer stress-strain curves of A7075.

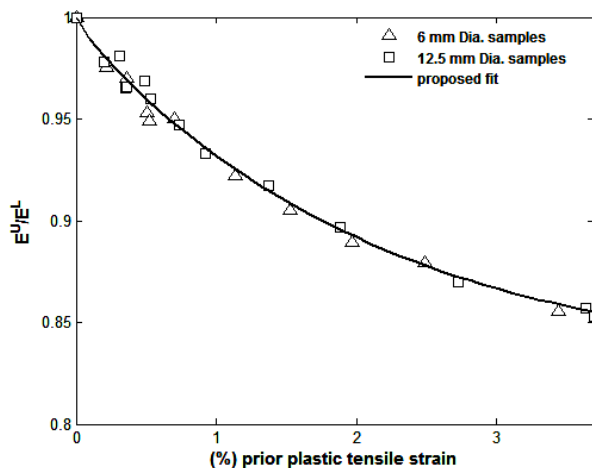


Figure 5. Experimental results and proposed fits for unloading Young's modulus in A7075.

4. 2. Investigating the Yield Strength

To investigate the plasticity problems, a precise definition of yield point (zero offset) is needed. This point usually is defined as the amount of plastic strain offset. The amount of plastic strain offset is usually calculated as 1% or 2% in engineering applications [7]. Perry et al. [7] investigated different methods of determining the yield point with different offsets and defined a new method called exact zero offset yield point. In this method, the yield point is obtained using knee-point in tangential modulus curve.

Considering that in some materials tangential modulus curve suddenly does not change. On the other hand, performing experiments to attain more number of experimental samples points around the yield point is prohibitively costly. Hence, determining the yield point for such materials is not attainable by the mentioned method. Parker et al. [8] suggested using small offset of 0.01% to determine the yield strength, unless the material has a sharp yield point that is required to use the exact zero offset.

Table 3 illustrates the amount of yield strength σ_Y for A7075 versus different offsets for both specimens. The results show that the amount of offset is an important factor in determining the yield strength of A7075. For different amounts of offset, various magnitudes are obtained for yield strength. The reason is the nonlinear behavior of the transmitting part A-B in A7075. Thus, the average amount of yield strength of A7075 is 424 MPa for 0.01% offset.

4. 3. Investigating Bauschinger Effect on Yield Stress

The ratio of compression yield strength to the initial tensile yield strength is called Bauschinger effect factor, BEF. BEF has the most effect on modeling

TABLE 3. The yield strength (MPa) of A7075 per different amount of offsets

	Percentage of offset value				
	0.01%	0.03%	0.05%	0.1%	0.2%
6 mm in diameter	422.4	436.5	442.2	446.4	448.9
12.5 mm in diameter	424.9	438.9	444.5	448.4	450.7
Mean value	424	438	443.7	447.7	450

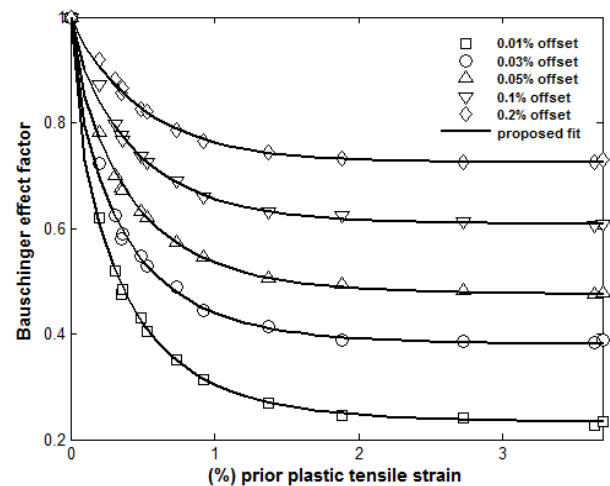


Figure 6. BEF of A7075 versus initial plastic strain; comparison different amounts of offset and proposed fits.

the behavior of high strength materials. This, in turn, decreases the useful effect of autofrettage. Therefore, careful analysis of autofrettage process requires accurate calculation of BEF. On the other hand, the amount of offset has great effect on determining the strength of tension-compression yield, and consequently affecting BEF.

Different ways of determining BEF were examined by Perry et al. [7, 16]. They defined the ratio of compression yield strength to the initial tensile yield strength with zero offset amounts to describe the BEF. Since reaching zero offset is too difficult or rather practically impossible, following the method of Parker et al. [8] and the study done in the Ref. [9], a very low offset amount of 0.01% is used for description of BEF in A7075.

Figure 6 illustrates BEF of A7075 which is a function of initial plastic strain, in different percentages of offset. As shown in the graph, BEF has been decreased by the amount of increase in initial plastic strain and the amounts of decrease offset. Also, it moves to special limited amounts when e_{PL}^{L*} increases. In other words, the exact prediction of inversed yield in the autofrettage process is possible only by very low amounts of offset. Equation (7) shows the proposed fit

to experimental data for the description of Bauschinger effect factor in the A7075 for offsets of 0.01%, 0.03%, 0.05%, 0.1% and 0.2%.

$$BEF = 1.0 + a \operatorname{Tanh}(b(e_{PL}^{L*})^c) \quad (7)$$

where the parameters of a, b and c are as listed in Table 4.

Figures 7 and with the offsets of 0.03% and 0.05%, compare BEF in two aluminum alloys of A7075 and A5083, respectively.

As Figures 7 and 8 show, the BEFs in A7075 are usually less than in A5083. Also, from the two Figures it is obvious that the BEF decreases as the level of prior plastic strain increases and offset amount has significant effect on BEF for the two alloys.

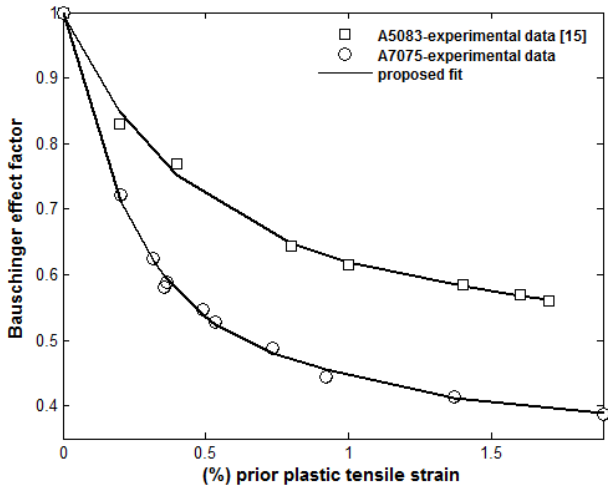


Figure 7. BEF changes versus initial plastic strain with the offset of 0.03%; the comparison between A7075 and A5083.

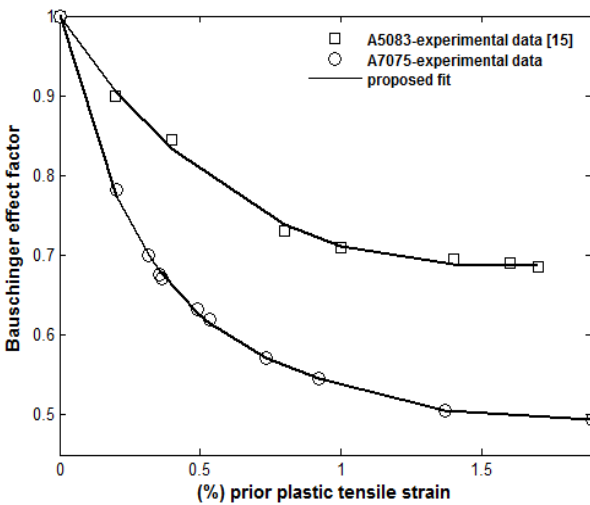


Figure 8. BEF changes versus initial plastic strain with the offset of 0.05%; the comparison between A7075 and A5083.

TABLE 4. Parameters of Equation (7)

Offset value	a	b	c
0.01%	-0.769	1.493	0.605
0.03%	-0.621	1.481	0.632
0.05%	-0.526	1.394	0.673
0.1%	-0.393	1.354	0.712
0.2%	-0.276	1.291	0.798

4. 4. Experimental Results and Proposed Mathematical Model

Figure 9 shows stress- strain plot of uniaxial A7075 test for total strains during loading-unloading cycle. It also shows the proposed fit based on Equations (1-4). The BEF is calculated based on 0.01% offset of experimental data. Then, it has been fit as function of e_{PL}^{L*} . As Figure 9 shows, there is a good agreement between proposed mathematical model and experimental results. Equations (8 and 9) are suggested to fit experimental data for modeling the A7075 behavior in the A-B-C and D-E-F regimes, respectively. These equations are presented as follows:

$$\sigma_{PL}^L / \sigma_Y = 0.128 \operatorname{Tanh}(8.402 e_{PL}^L) + 0.032 e_{PL}^L \quad (8)$$

$$\sigma_{PL}^L / \sigma_Y = (1 + 0.128 - BEF) \operatorname{Tanh}(\gamma e_{PL}^U) + BEF + 0.032 e_{PL}^U \quad (9)$$

In Equation (9), γ was suggested as nonlinear hardening strain for A7075 which is a function of maximum initial plastic strain e_{PL}^{L*} . It has been introduced in Equation (10).

$$\gamma = 1.41(e_{PL}^{L*})^{-0.13} \quad (10)$$

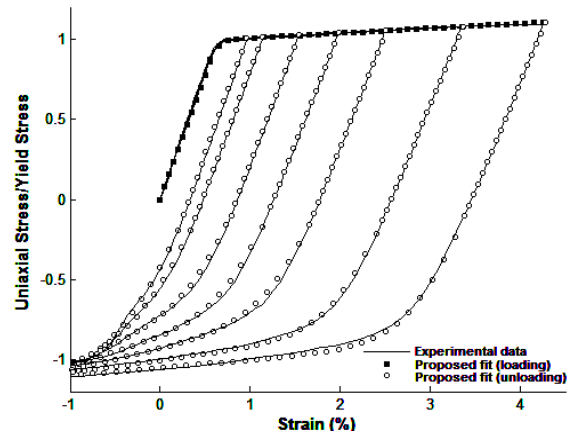


Figure 9. The mathematical complete model of A7075; the comparison between the results of experimental and proposed fits.

6. CONCLUSIONS

Uniaxial tension-compression tests for the modeling of A7075 behavior have been performed on specimens 12.5 mm and 6 mm in diameter using high accuracy Instron servohydraulic machine. Also, the results were compared with A5083 that led to the following conclusions:

1. The experimental results of both 6 mm and 12.5 mm specimens in uniaxial tension-compression are so close to each other that the differences are negligible.
2. Experimental data show that as the amount of initial plastic strain increases, the ratio of E^U/E^L in A7075 similar to many steels decreased, while the amount of elasticity modulus in aluminum alloys such as A5083 is equal in loading and unloading phases.
3. The fact that the amount of offset affects the yield strength in loading and unloading phases and also reaching at exact zero offset is difficult, it is suggested that minimum offset of 0.01% be used to determine the yield strengths of both phases.
4. Equation (7) with the determined factors fitted from experimental data show a proper correlation to describe BEF in A7075 that covers five offsets of 0.01%, 0.03%, 0.05%, 0.1% and 0.2%.
5. The experimental data show that for both aluminum alloys of A7075 and A5083, the amount of BEF decreases as the initial plastic strain increases. Also, the amount of offset has significant effect on BEF for the two alloys. The BEFs in A7075 are usually less than A5083 with the same level of prior plastic strains for different offsets.

7. ACKNOWLEDGMENTS

The writers of this research gratefully thank Mr. Zohrvand, the laboratory mechanical- property Technician of Amir- Kabir Industrial University for his great help in doing tests. The writers also specially thank Mr. Mehravaran, the Technician of Shahid Mohammad Montazeri University of Mashhad who helped a lot in preparing experimental specimens with high accuracy.

8. REFERENCES

1. Ma, Q., Levy, C. and Perl, M., "Stress intensity factors for partially autofretted pressurized thick-walled cylinders containing closely and densely packed cracks", *Journal of Pressure Vessel Technology*, Vol. 132, No. 5, (2010), 051203.
2. Mackerle, J., "Finite elements in the analysis of pressure vessels and piping, an addendum: A bibliography (2001–2004)", *International Journal of Pressure Vessels and Piping*, Vol. 82, No. 7, (2005), 571-592.
3. Herz, E., Thumser, R., Bergmann, J. and Vormwald, M., "Endurance limit of autofretted Diesel-engine injection tubes with defects", *Engineering Fracture Mechanics*, Vol. 73, No. 1, (2006), 3-21.
4. Perl, M., Levy, C. and Rallabhandy, V., "The influence of the Bauschinger effect on 3D stress intensity factors for internal radial cracks in a fully or partially autofretted gun barrel", *Journal of Pressure Vessel Technology*, Vol. 128, No. 2, (2006), 233-239.
5. Hill, R., "The mathematical theory of plasticity, Oxford university press, Vol. 11, (1998).
6. Bauschinger, J., "Ueber die Veränderung der Elasticitätsgrenze und dea Elasticitätsmoduls verschiedener Metalle", *Zivilingenieur*, Vol. 27, (1881), 289-348.
7. Perry, J., Perl, M., Shneck, R. and Haroush, S., "The Influence of the Bauschinger Effect on the Yield Stress, Young's Modulus, and Poisson's Ratio of a Gun Barrel Steel", *Journal of Pressure Vessel Technology*, Vol. 128, No. 2, (2006), 179-184.
8. Parker, A. P., Troiano, E., Underwood, J. H. and Mossey, C., "Characterization of steels using a revised kinematic hardening model incorporating Bauschinger effect", *Journal of Pressure Vessel Technology*, Vol. 125, No. 3, (2003), 277-281.
9. Farrahi, G., Hosseinian, E. and Assempour, A., "On the material modeling of the autofretted pressure vessel steels", *Journal of Pressure Vessel Technology*, Vol. 131, No. 5, (2009), 051403.
10. Troiano, E., Parker, A. P., Underwood, J. and Mossey, C., "Experimental data, numerical fit and fatigue life calculations relating to the Bauschinger effect in high strength armament steels", *Journal of Pressure Vessel Technology*, Vol. 125, No. 3, (2003), 330-334.
11. Megahed, M. and Abbas, A., "Influence of reverse yielding on residual stresses induced by autofretting", *International Journal of Mechanical Sciences*, Vol. 33, No. 2, (1991), 139-150.
12. Huang, X. and Cui, W., "Effect of Bauschinger effect and yield criterion on residual stress distribution of autofretted tube", *Journal of Pressure Vessel Technology*, Vol. 128, No. 2, (2006), 212-216.
13. Jahed, H. and Ghanbari, G., "Actual unloading behavior and its significance on residual stress in machined autofretted tubes", *Journal of Pressure Vessel Technology*, Vol. 125, No. 3, (2003), 321-325.
14. Jahed, H., Moghadam, B. A. and Shambooli, M., "Re-autofretting", *Journal of Pressure Vessel Technology*, Vol. 128, No. 2, (2006), 223-226.
15. Mohammadi, M., Farrahi, G. and Hoseini, S., "Bauschinger Effect Investigation of an Aluminum Alloy, and Its Application in Autofretted and Compound Tubes", in ASME Pressure Vessels and Piping Conference, American Society of Mechanical Engineers. (2007), 629-637.
16. Perry, J. and Aboudi, J., "Elasto-plastic stresses in thick walled cylinders", *Journal of Pressure Vessel Technology*, Vol. 125, No. 3, (2003), 248-252.

The Investigation of Modeling Material Behavior in Autofrettaged Tubes Made from Aluminium Alloys

K. Aliakbari, Kh. Farhangdoost

Department of Mechanical Engineering, Ferdowsi University of Mashhad, Mashhad, Iran

PAPER INFO

چکیده

Paper history:

Received 25 September 2012

Accepted in revised form 07 November 2013

Keywords:

Thick-Walled Tube

Autofrettage

Nonlinear Mathematical Model

Bauschinger Effect

Aluminum Alloys

در این تحقیق یک مدل ریاضی سخت‌شوندگی غیرخطی برای آلیاژ آلومینیم A7075 پیشنهاد می‌شود. به منظور تعیین مدل مناسب با لحاظ اثر باوشینگر از داده‌های تجربی آزمون‌های کشش-فشار تک محوره استفاده شد. از این رو، آزمون‌های کشش-فشار تک محوره روی تعدادی نمونه با قطرهای ۶ و ۱۲/۵ میلی‌متر به وسیله‌ی یک دستگاه سروهیدرولیک اینسترون انجام شد و با هم دیگر مقایسه شدند. در این مطالعه موارد مهمی از جمله مدول یانگ، مقدار افسست در تعیین نقطه‌ی تسلیم و ضریب اثر باوشینگر مورد مطالعه قرار گرفته است. علاوه بر این، ضریب اثر باوشینگر در دو آلیاژ آلومینیم A7075 و A5083 مورد استفاده در لوله‌ها مقایسه شدند. این مدل برای پیش‌گویی تنش پسماند و عمر خستگی در لوله‌های اتوفرتاژ شده به کار گرفته خواهد شد.

doi: 10.5829/idosi.ije.2014.27.05b.17
